




Overexpression of BUNDLE SHEATH DEFECTIVE 2 improves the efficiency of photosynthesis and growth in *Arabidopsis*

Florian A. Busch^{1,†} , Jun Tominaga^{2,†}, Masato Muroya^{2,†}, Norihiko Shirakami^{2,†}, Shunichi Takahashi^{1,‡}, Wataru Yamori³, Takuya Kitaoka⁴, Sara E. Milward¹, Kohji Nishimura⁵, Erika Matsunami⁵, Yosuke Toda³, Chikako Higuchi², Atsuko Muranaka², Tsuneaki Takami⁶, Shunsuke Watanabe^{2,§} , Toshinori Kinoshita^{4,7}, Wataru Sakamoto⁶, Atsushi Sakamoto² and Hiroshi Shimada^{2,*} 

¹Research School of Biology, Australian National University, Canberra, Australian Capital Territory 2601, Australia,

²Graduate School of Integrated Sciences for Life, Hiroshima University, 1-3-1 Kagamiyama, Higashi-Hiroshima 739-8526, Japan,

³Graduate School of Science, University of Tokyo, Bunkyo-ku, Tokyo 113-0033, Japan,

⁴Division of Biological Science, Graduate School of Science, Nagoya University, Chikusa, Nagoya 464-8602, Japan,

⁵Department of Molecular and Functional Genomics, Interdisciplinary Center for Science Research, Organization of Research, Shimane University, Nishikawatsu 1060, Matsue 690-8504, Japan,

⁶Institute of Plant Science and Resources, Okayama University, Kurashiki, Okayama 710-0046, Japan, and

⁷Institute of Transformative Bio-Molecules (WPI-ITbM), Nagoya University, Chikusa, Nagoya 464-8602, Japan

Received 22 February 2019; revised 1 November 2019; accepted 12 November 2019; published online 21 November 2019.

*For correspondence (e-mail hshimada@hiroshima-u.ac.jp).

†These authors contributed equally to this work.

‡Present address: Division of Environmental Photobiology, National Institute for Basic Biology, Okazaki 444-8585, Japan

§Present address: RIKEN Center for Sustainable Resource Science, Suehiro-cho, 1-7-22, Tsurumi-ku, Yokohama, Kanagawa 230-0045, Japan

SUMMARY

Bundle Sheath Defective 2, BSD2, is a stroma-targeted protein initially identified as a factor required for the biogenesis of ribulose 1,5-bisphosphate carboxylase/oxygenase (RuBisCO) in maize. Plants and algae universally have a homologous gene for BSD2 and its deficiency causes a RuBisCO-less phenotype. As RuBisCO can be the rate-limiting step in CO₂ assimilation, the overexpression of BSD2 might improve photosynthesis and productivity through the accumulation of RuBisCO. To examine this hypothesis, we produced BSD2 overexpression lines in *Arabidopsis*. Compared with wild type, the BSD2 overexpression lines *BSD2ox-2* and *BSD2ox-3* expressed 4.8-fold and 8.8-fold higher BSD2 mRNA, respectively, whereas the empty-vector (EV) harbouring plants had a comparable expression level. The overexpression lines showed a significantly higher CO₂ assimilation rate per available CO₂ and productivity than EV plants. The maximum carboxylation rate per total catalytic site was accelerated in the overexpression lines, while the number of total catalytic sites and RuBisCO content were unaffected. We then isolated recombinant BSD2 (rBSD2) from *E. coli* and found that rBSD2 reduces disulfide bonds using reductants present *in vivo*, for example glutathione, and that rBSD2 has the ability to reactivate RuBisCO that has been inactivated by oxidants. Furthermore, 15% of RuBisCO freshly isolated from leaves of EV was oxidatively inactivated, as compared with 0% in BSD2-overexpression lines, suggesting that the overexpression of BSD2 maintains RuBisCO to be in the reduced active form *in vivo*. Our results demonstrated that the overexpression of BSD2 improves photosynthetic efficiency in *Arabidopsis* and we conclude that it is involved in mediating RuBisCO activation.

Keywords: *Arabidopsis thaliana*, BSD2, disulfide bonds, oxidative stress, protein disulfide reductase, redox, RuBisCO, Zn finger domain.

INTRODUCTION

The first step of CO₂ fixation is catalyzed by ribulose 1,5-bisphosphate carboxylase/oxygenase (RuBisCO) in the chloroplast stroma, and is often the rate-limiting step of photosynthesis in the natural environment (Sage *et al.*,

2008). RuBisCO is required in high amounts in C₃ plant chloroplast due to its low catalytic turnover rate and limited specificity for CO₂ versus O₂ (Parry *et al.*, 2013). Therefore, RuBisCO has been targeted to be artificially modified to improve photosynthesis and plant productivity.

However, manipulations of RuBisCO in either catalytic properties or quantity are not straightforward partly because putting 16 protein subunits together ($L_8:S_8$; eight large and eight small subunits) in one RuBisCO is a complex task requiring numerous chaperones (Whitney *et al.*, 2011; Aigner *et al.*, 2017). Furthermore, auxiliary factors are also required for the activation of mature RuBisCO, imposing additional limitations on the apparent catalytic performance (Portis, 2003; Sage *et al.*, 2008).

RuBisCO activity is determined in a light-dependent manner and is active in the light and inactive in the dark. Sequential binding of CO_2 and Mg^{2+} is a pre-requisite for RuBisCO catalysis (Portis, 2003). This process is inhibited by a range of sugar phosphates that tightly bind to the active site in the large subunit. Upon illumination, ATP-dependent RuBisCO activase promotes RuBisCO activation by releasing these ligands when the stromal ATP/ADP ratio increases with photophosphorylation (Scales *et al.*, 2014). Active photosynthetic electron transport also triggers the release of Mg^{2+} from the thylakoid to the stroma pool, thereby facilitating RuBisCO activation.

Aside from its regulation by carbamylation, RuBisCO activity is also redox regulated. It has been shown that reactive oxygen species (ROS), such as hydrogen peroxide (H_2O_2), inactivate RuBisCO (Moreno *et al.*, 2008). The production of ROS is accelerated in conditions where the absorbed light energy is excessive for photosynthesis, for example during environmental stress. Therefore, it is assumed that RuBisCO tends to be inactivated by ROS under such stressful conditions (Zaffagnini *et al.*, 2012). In laboratory experiments, the oxidatively inactivated RuBisCO has been demonstrated to be reactivated by the addition of reducing agents, for example dithiothreitol (DTT), indicating that this inactivation is reversible (Sudhani and Moreno, 2015). However, it is unknown if oxidatively inactivated RuBisCO is reactivated *in vivo* or if any enzyme is involved in this process.

BUNDLE SHEATH DEFECTIVE2 (BSD2), a small stroma-targeted protein, was initially identified as an essential factor for RuBisCO biogenesis in maize (Brutnell *et al.*, 1999), and now appears to be universal in green algae and plants (Doron *et al.*, 2014; Aigner *et al.*, 2017). BSD2-deficient plants cannot accumulate the large subunit of RuBisCO despite its active translation and transcription (Brutnell *et al.*, 1999; Wostrickoff and Stern, 2007). Several studies have proposed that BSD2 acts in post-translational modification of nascent large subunit or RuBisCO assembly (Brutnell *et al.*, 1999; Wostrickoff and Stern, 2007; Doron *et al.*, 2014; Aigner *et al.*, 2017). The recent success in recombinant expression of plant RuBisCO in *Escherichia coli* identified BSD2 as the late-stage assembly factor which seems to stabilize the premature L_8 complex (Aigner *et al.*, 2017). This view is consistent with the protein annotation of BSD2 homologues, which uniquely conserve the cysteine

(Cys) rich Zn finger domains of the DnaJ chaperone in *E. coli* (Brutnell *et al.*, 1999).

As BSD2 was shown to be involved in the production and accumulation of RuBisCO in plants it is conceivable that overexpression of BSD2 improves photosynthesis and productivity through accumulating RuBisCO. Conlan *et al.* (2018) recently showed that overexpressing BSD2 in tobacco chloroplasts did not alter RuBisCO content, activation status, leaf photosynthesis rate, or plant growth. Here, we produced BSD2-overexpressing lines, *BSD2ox-2* and *BSD2ox-3*, in Arabidopsis. Our results demonstrate that the overexpression of BSD2 increases the CO_2 assimilation rate and plant biomass by increasing the maximum carboxylation rate by increasing the proportion of active catalytic sites, but not by increasing the number of total catalytic sites or RuBisCO content. To understand its mechanism, we isolated recombinant BSD2 (rBSD2) from *E. coli* and found that BSD2 has the ability to reactivate oxidatively inactivated RuBisCO *in vitro*. In this study, we examined how overexpression of BSD2 improves photosynthesis and productivity and discuss a physiological function of BSD2 in plants. Our results demonstrated that BSD2 is a key component in the mechanism to reactive oxidized RuBisCO, thereby maintaining photosynthetic efficiency in plants.

RESULTS

Overexpression of BSD2 improves photosynthetic efficiency and increases plant biomass

The full-length open reading frame of BSD2 cDNA was used to generate an overexpression vector pG2CYO2. Following floral dipping, transgenic Arabidopsis plants were selected on both kanamycin-containing and hygromycin-containing medium (Nakagawa *et al.*, 2007). We isolated 15 BSD2-overexpressing lines, and the two lines (*BSD2ox-2* and *BSD2ox-3*) showing the highest levels of BSD2 (At3g47650) transcripts at T3 generation were selected for this study. The levels of BSD2 transcripts in *BSD2ox-2* and *BSD2ox-3* were 4.8-fold and 8.8-fold higher than in the wild type, respectively, and there was no significant difference between wild type and the empty-vector control (Figure 1a). Along with their higher BSD2 gene expression, the *BSD2ox* lines accumulated 74–78% more BSD2 protein in leaves than the control plants (Figure 1b). Conversely, the results of SDS-PAGE analysis indicated the amounts of both RuBisCO large and small subunits were comparable between the *BSD2ox* and control leaves (Figure 1c; Figure S1). Nevertheless, the *BSD2ox* lines increased their leaf area relative to the control (Figure 1d; Figure S2). The increased leaf area was due to an increase in the size of individual leaves (Figure 1e; Figure S3) but not the number of leaves (Figure S4). Eventually, the *BSD2ox* lines had a 1.23–1.35-fold larger shoot dry mass than the control at 35

days after seeding (Figure 1e). In gellan gum-grown plants, the shoot/root ratio was similar between the *BSD2ox* lines and control (Figure S5), suggesting that the carbon-partitioning was unaltered.

To see the effect of overexpression of *BSD2* on photosynthesis, CO₂ assimilation rate per leaf area (*A*) in response to varying CO₂ concentrations was measured under saturating irradiance. The response of *A* to the CO₂ concentration in either the intercellular airspace (*C_i*;

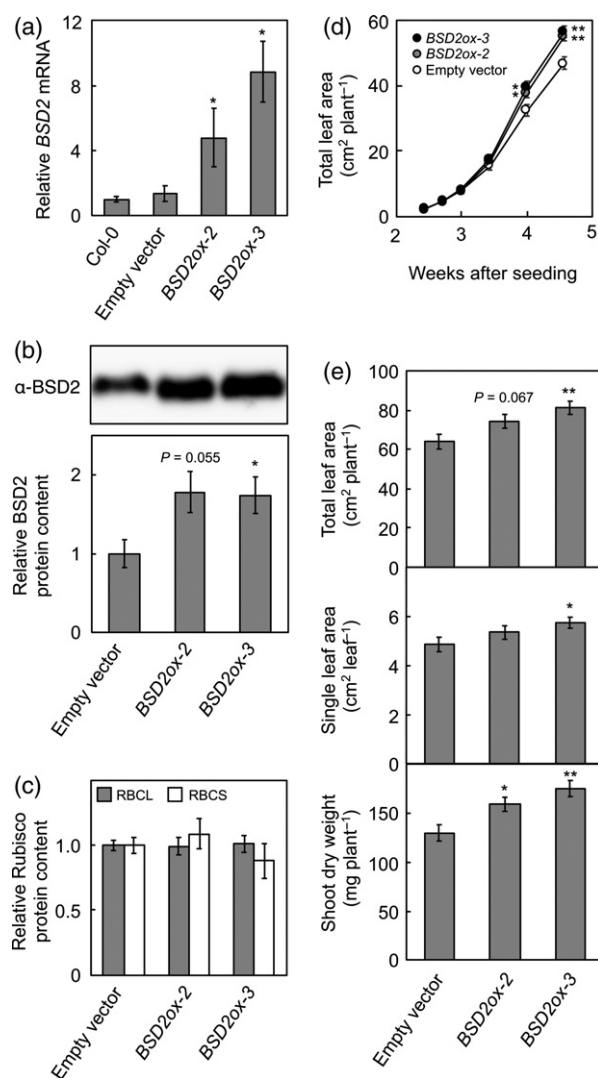


Figure 1. Gene expression, protein accumulation, and growth in wild type (Col-0) and transgenic plants transformed either with an empty vector (*Empty vector*) or the *BSD2* overexpression vector (*BSD2ox-2*, *BSD2ox-3*). (a) Expression of *BSD2* gene transcript in leaves of 3-week-old transgenic lines relative to Col-0 (mean \pm SE; $n = 4$). (b) Western blotting analysis for BSD2 protein in leaves of 3-week-old plants. Values relative to Col-0 are shown (mean \pm SE; $n = 3$). (c) SDS-PAGE analysis for large and small subunits of RuBisCO (RBCL and RBCS) in leaves of 3-week-old plants. Relative values to Col-0 are shown (mean \pm SE; $n = 6$). (d) Change of total leaf area at 2 and 5 weeks after seeding (mean \pm SE; $n = 7$). (e) Total leaf area per plant, average leaf area per individual leaf, and shoot dry weight of 35-day-old plants (mean \pm SE; $n = 7$). *P*-values by Student's *t*-test are indicated if less than 0.1 (**P* < 0.05, ***P* < 0.01).

Figure S6) or at the site of carboxylation (*C_i*; Figure 2a) showed greater photosynthetic capacity in the *BSD2ox* leaves. Fitting a photosynthetic model to these *A*-*C_i* plots, we estimated the maximum RuBisCO carboxylation rate (*V_{cmax}*) and the photosynthetic electron transport rate (*J*) (Figure 2b). The *BSD2ox* leaves had higher *V_{cmax}* than control leaves by 19–26%. *J* also tended to be higher in the *BSD2ox* leaves, resulting in similar *J/V_{cmax}* ratios (Figure 2b). This indicates that photosynthetic electron transport capacity is increasing in parallel with *V_{cmax}* in the *BSD2ox* plants. It is therefore likely that the increase in biomass in the *BSD2ox* plants is caused by this increase in photosynthetic capacity. Furthermore, the number of RuBisCO total catalytic sites *per* leaf area in those leaves for the photosynthesis measurements was not significantly different between the overexpression lines and control (Figure 2c). Nevertheless, the apparent catalytic efficiency for RuBisCO carboxylation, estimated as *V_{cmax}* *per* total catalytic site, was higher in the *BSD2ox* lines (Figure 2c). This indicates that proportion of active catalytic sites to total catalytic sites of RuBisCO was increased in the *BSD2ox* leaves. Overall, *in vivo* catalytic efficiency rather than RuBisCO content was enhanced in the *BSD2ox* leaves, resulting in higher overall photosynthetic capacity and growth.

BSD2 catalyzes reduction of disulfide bonds

To understand how the overexpression of BSD2 enhanced the catalytic efficiency for RuBisCO carboxylation *in vivo*, we isolated rBSD2 protein from *E. coli* and studied its characteristics. BSD2 orthologues in green plants contain two Cys4-type Zn finger motifs (CXXCXGXG) (Brutnell *et al.*, 1999; Wostrikoff and Stern, 2007; Doron *et al.*, 2014), which show either chaperone activity or thiol-disulfide oxidoreductase activity in *E. coli* DnaJ (Tang and Wang, 2001). In chloroplasts, four other proteins likewise contain a DnaJ-like domain: CYO1/SCO2 (Shimada *et al.*, 2007; Albrecht *et al.*, 2008), LQY1 (Lu *et al.*, 2011) and HCF222 (Hartings *et al.*, 2017) in/at the thylakoid membrane, and PSA2 in the thylakoid lumen (Fristedt *et al.*, 2014). They all exhibit protein disulfide reductase (PDR) activity like DnaJ (de Crouy-Chanel *et al.*, 1995). We then tested whether rBSD2 also has PDR activity with a protein disulfide isomerase (PDI) assay (Raturi and Mutus, 2007; Muranaka *et al.*, 2012). In this assay, fluorescence increases if the reduction of disulfide bonds is mediated by diethylenetriamine glutathione (Di-E-GSSG). When purified rBSD2 and a non-specific reductant (i.e. DTT) was added to PDI assay solution containing Di-E-GSSG, the fluorescence signal significantly increased (Figure 3a). However, such an increase did not happen in the presence of DTT without rBSD2. These results demonstrate that rBSD2 has PDR activity, which is further supported by the dependency of the reaction rate on the substrate concentration (Figure 3b).

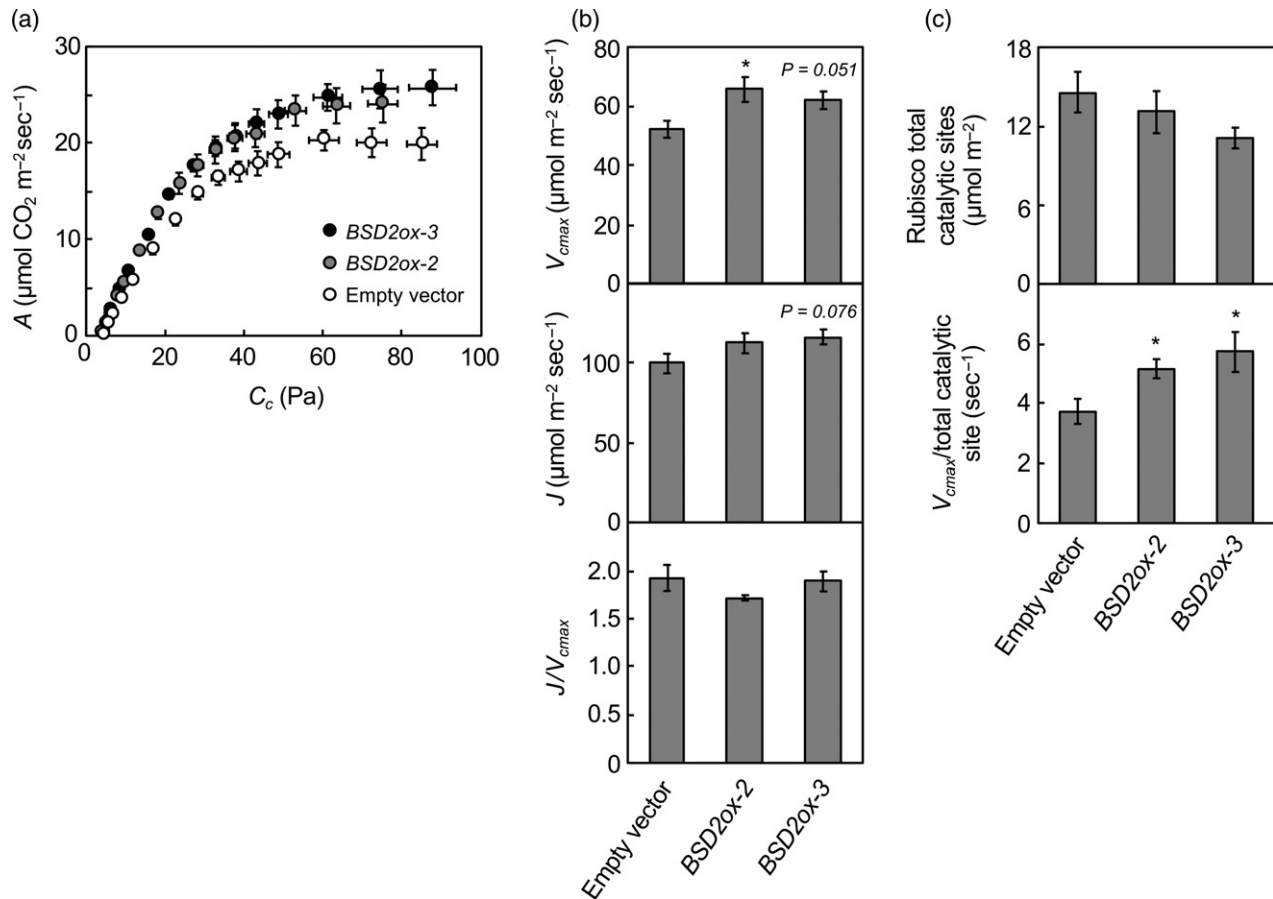


Figure 2. Photosynthesis in leaves of empty-vector control plants (*Empty vector*) and *BSD2*-overexpressing plants (*BSD2ox-2,3*). (a) Response of CO₂ assimilation (*A*) to chloroplastic CO₂ concentration in leaves (*C_c*) (mean ± SE; *n* = 4–5). (b) Maximum RuBisCO carboxylation rate (*V_{cmax}*) and photosynthetic electron transport rate (*J*) fitted to the *A*–*C_c* response curves in (a), and the *J/V_{cmax}* ratio. (c) Number of RuBisCO total catalytic sites per leaf area, and the maximum RuBisCO carboxylation rate (*V_{cmax}*) per total catalytic site (mean ± SE; *n* = 4–5). Both *V_{cmax}* in (b) and total catalytic sites in (c) were measured in the same leaves as used in (a). *P*-values by Student's *t*-test are indicated if less than 0.1 (**P* < 0.05).

Each of CYO1, LQY1, HCF222 and PSA2 is associated with membrane-embedded photosynthetic complexes involved in thylakoid biogenesis/homeostasis (Lu *et al.*, 2011; Muranaka *et al.*, 2012; Tanz *et al.*, 2012; Fristedt *et al.*, 2014). Considering BSD2 is a stromal protein, we expect that the catalytic properties of BSD2 are different from the membrane-embedded proteins. We then estimated PDR kinetics of rBSD2 from the Michaelis–Menten curve (Figure 3b), as was done for the recombinant CYO1 in *Arabidopsis* (Muranaka *et al.*, 2012) and rice (Tominaga *et al.*, 2016). *K_m* and *K_{cat}* values for rBSD2 were 9.19 μM and 3.39 min⁻¹, respectively, which are higher than those of CYO1 (Table 1), suggesting that BSD2 has a lower affinity for its substrate. This distinctive feature may reflect differences in accessibility to and/or abundance of their substrates in the highly crowded macromolecular solution.

PDR activity of rBSD2 relies on the presence of reductant. To examine whether rBSD2 can use biological reductants, we measured the PDR activity of rBSD2 in the presence of reduced glutathione (GSH), NADPH, or NADH.

Our results demonstrated that GSH is the most effective reductant among them and its efficiency is comparable to DTT (Figure 3c).

BSD2 reactivates oxidized RuBisCO

Previous studies have demonstrated that RuBisCO loses activity through the oxidation of its cysteine residues (Marcus *et al.*, 2003; Moreno *et al.*, 2008). We therefore tested whether BSD2 can reduce and thereby reactivate oxidized RuBisCO. Carboxylation rates of purified RuBisCO decreased by 60% after being oxidized with 5 mM H₂O₂ (Figure 4a). We then tested the effect of rBSD2 on the recovery of the carboxylation rate in the presence of 1 mM DTT. In our experimental condition, the carboxylation rate did not change in the absence of rBSD2, although higher concentrations of DTT might be able to reactivate oxidized RuBisCO (Sudhani and Moreno, 2015). However, in the presence of rBSD2, the rate partially, but significantly, recovered (Figure 4b). Our results demonstrate that rBSD2 can reactivate oxidized RuBisCO.

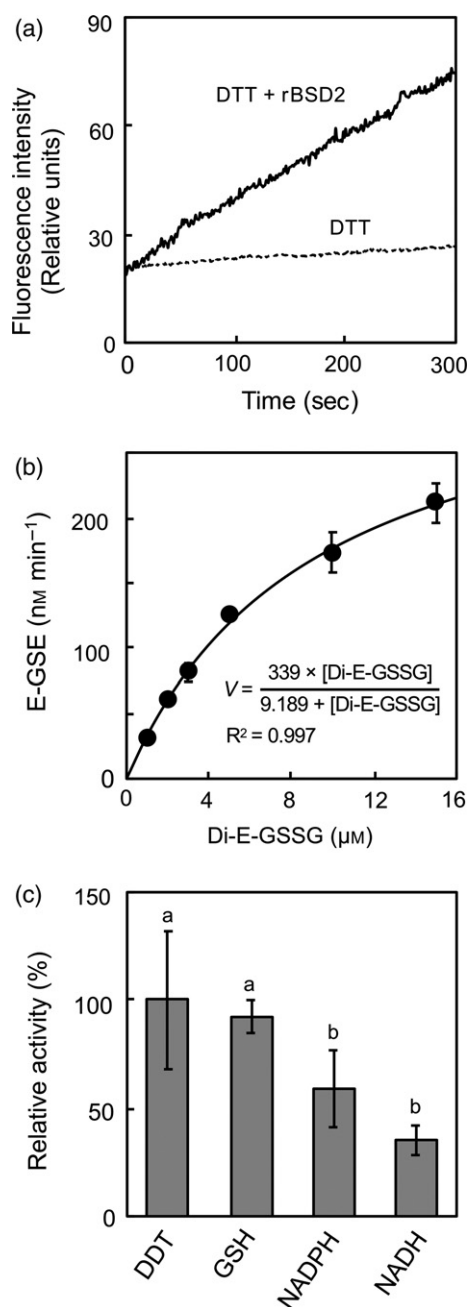


Figure 3. PDR assay of rBSD2. (a) Change in fluorescence intensity after a solution containing 1 μM Di-E-GSSG was incubated with 5 μM DTT in the presence (solid line) or absence (broken line) of 100 nM rBSD2. (b) Michaelis–Menten curve for PDR kinetics with 5 μM DTT. K_m and V_{max} of rBSD2 were estimated to be 9.189 μM and 339 nm min^{-1} , respectively (mean \pm SD; $n = 3$). (c) Effect of 5 μM reductants on the PDR activity. Values relative to DTT are shown (mean \pm SD; $n = 3$). Different letters indicate significant difference among reductants (Tukey's test, $P < 0.05$).

To examine whether the overexpression of BSD2 influences the redox state of RuBisCO in leaves, we isolated crude protein samples from leaves without adding reductants and subsequently measured the RuBisCO carboxylation rate after incubating the sample with or without DTT

Table 1 Kinetic properties of BSD2 and CYO1 in *Arabidopsis thaliana* and *Oryza sativa*. Data for CYO1 were obtained in previous studies (Muranaka *et al.*, 2012; Tominaga *et al.*, 2016)

	Species	K_m (μM)	K_{cat} (min^{-1})	$K_{\text{cat}} K_m^{-1}$ ($\times 10^3 \text{M}^{-1} \text{sec}^{-1}$)
BSD2	<i>A. thaliana</i>	9.19 ± 0.93	3.39 ± 0.16	6.2 ± 0.8
CYO1	<i>A. thaliana</i>	0.82 ± 0.09	0.53 ± 0.02	10.7 ± 1.5
	<i>O. sativa</i>	3.16 ± 0.88	0.53 ± 0.05	2.8 ± 0.4

Means \pm SE ($n = 3$).

for 30 min. In the empty-vector control, the RuBisCO carboxylation rate in samples incubated with DTT was 15% higher than when incubated without DTT, indicating that 15% of RuBisCO catalytic sites was inactive due to oxidation (Figure 5). Conversely, RuBisCO carboxylation rate in the BSD2 overexpression lines could not be increased by adding the reductant DTT, showing that there was no activity loss due to oxidation in the extracted protein samples (Figure 5). Our results demonstrated that RuBisCO from freshly isolated leaves consists of a higher proportion of the reduced active form in the BSD2 overexpression lines than in the control.

DISCUSSION

Our results demonstrate that BSD2 overexpression improves both photosynthesis and productivity in our study organism *Arabidopsis*. BSD2 overexpression did not change the RuBisCO content or the number of total catalytic sites, but improved the *in vivo* maximum carboxylation efficiency probably through increasing the pool of reduced RuBisCO.

Incubation of isolated RuBisCO in oxidants, including ROS, decreases RuBisCO activity (Marcus *et al.*, 2003). The

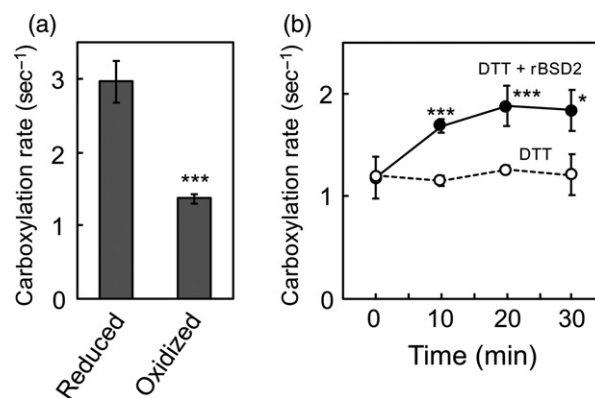


Figure 4. RuBisCO reactivation assay. (a) RuBisCO carboxylation rate after incubation with 1 mM DTT (reduced) or 5 mM H_2O_2 (oxidized) for 30 min (mean \pm SD; $n = 3$). (b) Change in carboxylation rate of the pre-oxidized 80 nM RuBisCO in the presence (closed circles) or absence (open circles) of 40 nM rBSD2 (mean \pm SD; $n = 3$). ($*P < 0.05$, $***P < 0.001$, by Student's *t*-test).

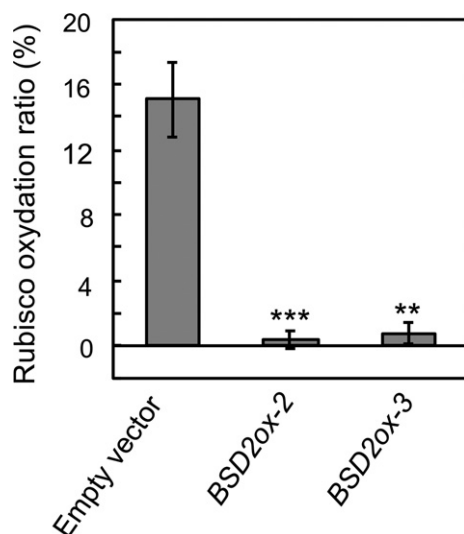


Figure 5. Redox-dependent inactivation of RuBisCO. The RuBisCO oxydation ratio was calculated as a remaining proportion of the RuBisCO carboxylation rate estimated without DTT present (w/o DTT) relative to that with DTT present (w DTT) $\left[\left(1 - \frac{w/o DTT}{w DTT} \right) \times 100 \right]$. Means \pm SE ($n = 3$) are shown. (** $P < 0.01$, *** $P < 0.001$, by Student's *t*-test).

oxidatively inactivated RuBisCO has been demonstrated *in vitro* to be reactivated by reductants, such as DTT (García-Ferris and Moreno, 1993; Marcus *et al.*, 2003; Sudhani and Moreno, 2015). In the present study, we demonstrated that rBSD2 can reactivate the oxidatively inactivated RuBisCO and can act as a catalyst for this reduction. As a consequence, photosynthetic efficiency is improved despite no observed increase in absolute RuBisCO content. This is consistent with results showing that the overexpression of BSD2 increases the apparent carboxylation efficiency of RuBisCO (Figure 2) and that the reduced form of RuBisCO was more abundant in the BSD2 overexpression lines than in the control (Figure 5). However, we need to note that the effect of overexpression of BSD2 on the RuBisCO catalysis and photosynthesis might differ among plants and environments, depending on the sensitivity of RuBisCO to the oxidants, such as ROS. Indeed, the overexpression of BSD2 has not improved photosynthesis in tobacco (Conlan *et al.*, 2018).

PDR activity of BSD2 reactivates oxidatively inactivated RuBisCO

Oxidation of RuBisCO by oxidants, including ROS, inactivates RuBisCO, but its mechanism remained unknown. However, as RuBisCO possesses cysteine residues that are sensitive to oxidants, it is conceivable that the oxidation of cysteine residues is associated with the inactivation of RuBisCO. Importantly, RuBisCO oxidized by disulfides such as cystamine can be reactivated by thiols like DTT and cysteamine (García-Ferris and Moreno, 1993; Marcus *et al.*, 2003; Sudhani and Moreno, 2015). Therefore, the

inactivation of RuBisCO by oxidants is reversible, most likely through the reduction of oxidized cysteine residues. In the present study, we showed that rBSD2 has PDR activity, suggesting that reactivation of oxidatively inactivated RuBisCO by BSD2 is associated with the direct thiol transactions between oxidized RuBisCO and BSD2. In practice, this reaction occurs only if effective reductants are available at the site of RuBisCO (i.e. in the stroma). We confirmed that glutathione, NADPH, and NADH, which also exist in the stroma, could initiate the PDR reaction and that glutathione was the most effective of these reductants (Figure 3c). A similar preference for reductants has also been observed in CYO1 (Muranaka *et al.*, 2012; Tominaga *et al.*, 2016). It is known that RuBisCO is a potential target of both thioredoxins (Balmer *et al.*, 2004; Lemaire *et al.*, 2004) and glutaredoxins (Zaffagnini *et al.*, 2012). Although thioredoxins can target vicinal Cys pairs of RuBisCO, they are unlikely to be involved in the reactivation as these disulfides are not critical for the catalytic activity (Ranty *et al.*, 1991; Moreno and Spreitzer, 1999; Marín-Navarro and Moreno, 2006), and the concentration of thioredoxins is not sufficient to reduce the large pool of RuBisCO (Peltier *et al.*, 2006; Sudhani and Moreno, 2015). Conversely, glutathione and ascorbate are very abundant in the chloroplast stroma ranging between 0.5–3.5 and 20–300 mM, respectively, thereby constituting a pool of redox buffers against oxidants (Foyer and Noctor, 2011; Dietz *et al.*, 2016). In contrast with the light-dependent ferredoxin–thioredoxin system, the glutathione pool (i.e. GSH/GSSG ratio) may not be oxidized very much when photosynthetic electron transport is low (e.g. in the dark, under stress conditions, and during senescence) owing to decreased metabolic demands and catabolic supply of reducing equivalents (Foyer and Noctor, 2011). Therefore, chloroplastic glutathione would allow BSD2 to continuously reduce, and thereby maintain RuBisCO to be in the active form (Sudhani and Moreno, 2015). It is noteworthy that a drop in the GSH/GSSG ratio in response to excess ROS may cause a translational arrest of the RuBisCO large subunit, related to oxidation of the nascent polypeptide (Irihimovitch and Shapira, 2000).

In our experiments, rBSD2 reactivated oxidatively inactivated RuBisCO, but the RuBisCO activity did not recover to the initial level (Figure 4). This result suggests that the oxidatively inactivated RuBisCO includes reversible and irreversible states. Previous studies have demonstrated that the oxidation of RuBisCO decreases the number of catalytic sites, resulting in an irreversible deactivation (Marcus *et al.*, 2003). Furthermore, it has been demonstrated that ROS can cause direct fragmentation of the large subunit *in vitro* (Ishida *et al.*, 1998) and in intact chloroplasts (Nakano *et al.*, 2006). The unrecoverable activity of H₂O₂-oxidized RuBisCO after BSD2 treatment (Figure 4b) might therefore represent either irreversible

conformational change or decomposition of the RuBisCO complex.

Physiological function of BSD2 *in vivo*

It has been widely accepted that BSD2 is a critical chaperone in RuBisCO assembly in plants and green algae. During RuBisCO biogenesis BSD2 appears to function in preventing an end-state assembly intermediate from the aggregation until the small subunits become available (Brutnell *et al.*, 1999; Wostrickoff and Stern, 2007; Aigner *et al.*, 2017). It has also been suggested that BSD2 is a co-translational chaperone that protects nascent large subunit chains from misfolding (Doron *et al.*, 2014). Here, we confirmed the hypothesis that BSD2 may also target the post-assembled RuBisCO and reactivate oxidatively inactivated RuBisCO. It has been frequently noted that oxidation of RuBisCO is physiologically relevant to senescence or stress scenarios, which are known to trigger a fast catabolism of RuBisCO (García-Ferris and Moreno, 1993; Moreno and Spreitzer, 1999; Marcus *et al.*, 2003; Marín-Navarro and Moreno 2003). The reactivation of RuBisCO by BSD2 might be therefore important for alleviating senescence or stress scenarios, as well as for maintaining functional photosynthesis.

EXPERIMENTAL PROCEDURES

Plant materials and growth conditions

The full-length open reading frame of BSD2 cDNA was used to generate an overexpression vector pG2CYO2. The full-length ORF of BSD2 cDNA was amplified using primers At3g47650-F-attB1 (5'-AAAAGCAGGCTATATGGCGAATTCATGCTTCTTCTCTCC-3') and At3g47650-attB2 (5'-AGAAAGCTGGTACTCATGAAGGTGCTCAAGAACCACC-3'). The resulting amplified product was cloned into pDONR/Zeo (Invitrogen, ThermoFisher, Carlsbad, CA, USA) to make pD3gORFull, and the sequence was confirmed. The full-length ORF was introduced into the pGWB2 Gateway vector (Nakagawa *et al.*, 2007) by recombination from the pD3gORFull to make pG2BSD2. The pG2BSD2 vector was introduced into wild type *Arabidopsis thaliana* (Columbia-0) by floral dipping (Clough and Bent, 1998) using *Agrobacterium tumefaciens* GV3101. Fifteen transgenic lines were obtained, and T3 was used for the study.

Plants were grown at 22–23°C, 60–85% (relative humidity) under a 16-h fluorescent light (100 $\mu\text{mol m}^{-2} \text{sec}^{-1}$)/8-h dark cycles on $\frac{1}{2}$ MS plates or in soil.

Photosynthesis measurements

Photosynthetic gas exchange of 5-week old Col-0 and BSD2 overexpression plants were measured using a Licor 6400XT gas exchange system equipped with a leaf chamber fluorometer (LICOR, Lincoln, Nebraska USA). Measurements were performed at a leaf temperature of 25°C and a VPD of 1 kPa. CO_2 response curves were measured at a saturating light intensity of 1200 $\mu\text{mol m}^{-2} \text{sec}^{-1}$. The curves were fitted for V_{cmax} , J , and g_m with the Excel fitting tool provided by Sharkey *et al.* (2007), which was parameterized with the RuBisCO kinetic parameters of Arabidopsis described elsewhere (Walker *et al.*, 2013). CO_2 concentrations at the site of carboxylation (C_c) were calculated according to Fick's law as $C_c = C_i - A/g_m$.

SDS-PAGE and immunoblot analysis

Rosette leaves (100 mg fresh weight) from each 3-week-old plant were ground with a mortar and pestle in liquid nitrogen and transferred to a new 1.5-ml tube and homogenized in 5 volumes (v/w) of extraction buffer containing 15 mM Tris-HCl, pH 8.0, 50 mM NaCl, 10 mM ethylenediaminetetraacetic acid (EDTA) and 1.0% protease inhibitor cocktail (Sigma-Aldrich, Tokyo, Japan). The samples were incubated on ice 10 min with vigorous vortexing every minute and centrifuged (20 000 g , 20 min, 4°C). The supernatant equivalent of 1.5 mg of fresh weight was electrophoresed on a 16.5% Tris-tricine SDS-PAGE gel and electroblotted onto polyvinylidene difluoride (PVDF) membrane. The membrane was immunoreacted with anti-BSD2 antibody (a kind gift from Spencer M. Whitney, Australian National University) and detected using an ECL Select kit (GE Healthcare, Chicago, IL, USA). Ribulose 1,5-bisphosphate carboxylase/oxygenase subunits RBCL and RBCS were visualized by staining the gel with Coomassie Brilliant Blue R250.

Expression and purification of the rBSD2 protein

Truncated BSD2 cDNA was amplified by reverse transcriptase polymerase chain reaction (RT-PCR) using primers that contained sites for *NdeI* (At3g47650-*Nde*, 5'-GGGCATATGGCCGCAACAA TAATCCTCAGGGCACTAAACC-3') and *XhoI* (At3g47650-*Xho*, 5'-CCCTCGAGCTCATGAAGGTGCTCAAGAACCACC-3'). The amplified DNA fragments encoded the BSD2 protein containing amino acids 57 to 136. The DNA fragments were digested with *NdeI* and *XhoI* and ligated into the expression vector pET-24b(+) (Novagen, Sigma-Aldrich, St. Louis, MD, USA). The sequence of the DNA fragment was confirmed. The *E. coli* strain BL21(DE3) was used for expression of the truncated BSD2 fusion proteins with 6 \times His tags. Overnight cultured BL21(DE3) cells harbouring the truncated BSD2 gene were diluted 1:20 with fresh culture medium and grown at 37°C for 1 h. Isopropyl- β -D-thiogalactopyranoside was then added to a final concentration of 1.0 mM, and the cells were cultured at 20°C overnight. The cells were centrifuged for 10 min at 5000 g and 4°C. The cell pellets were suspended in suspension buffer (15.0 mM Tris-HCl, pH 7.0, 50.0 mM NaCl, 0.1 mM DTT, and 1.0 mM phenylmethylsulfonyl fluoride). The cells were sonicated and the crude extract centrifuged for 10 min at 12 000 g and 4°C. The supernatant was incubated for 1 h with nickel-nitrilotriacetic acid agarose (Qiagen, Venlo, the Netherlands) at 4°C. The agarose was washed with suspension buffer containing 30 mM imidazole. rBSD2 protein bound to the agarose was eluted with suspension buffer containing 200 mM imidazole. The eluted proteins were dialyzed with phosphate-buffered saline buffer at 4°C overnight.

Assay for PDR-dependent disulfide reduction

Dieosin glutathione disulfide, Di-E-GSSG, was prepared as described in previous study (Muranaka *et al.*, 2012). PDI disulfide reduction assay was conducted in PDI assay buffer (100 mM potassium phosphate, pH 7.0) containing 100 nM rBSD2 and Di-E-GSSG (100–1500 nM) with 5 μM DTT. The increase in fluorescence at 545 nm was monitored with excitation at 525 nm. The kinetic parameters were calculated using KaleidaGraph software (Synergy Software, Reading, PA, USA).

RuBisCO purification and assay

Leaves from 4-week-old Arabidopsis plants were frozen in liquid nitrogen, and RuBisCO was purified by ion-exchange chromatography (Sharwood *et al.*, 2008) as follows. The frozen leaves were homogenized in glass homogenizer in ice-cold 50 mM Tris-HCl pH

7.6, 1 mM EDTA, 1% (w/v) polyvinylpyrrolidone, 5 mM DTT, plant protease inhibitor cocktail (Sigma, St. Louis, MD, USA, Product # P9599; 200 μ l per 25 ml solution), then centrifuged at 16 000 g for 15 min at 4°C. Next, the supernatant was added to a 5-ml Bio-Scale Mini Macro-prep High Q cartridge (Bio-Rad, Hercules, CA, USA) equilibrated with 50 mM Tris-HCl, pH 7.6, 1 mM EDTA under the control of an AKTA chromatography system. The elution system consisted of a 35-ml gradient of a 0–1 M NaCl at a flow rate of 2 ml min^{-1} , and 2-ml fractions were collected. Fractions containing RuBisCO activity (determined by the $^{14}\text{CO}_2$ RuBisCO activity assay described below) were pooled and dialyzed overnight at 4°C against 1 L of 50 mM Tris-HCl, pH 7.6, 1 mM EDTA, 20% (v/v) glycerol. Aliquots were frozen in liquid nitrogen and stored at -80°C . Before the RuBisCO activity assay, purified RuBisCO was activated in 50 mM EPPS-NaOH, pH 8.0, 15 mM NaHCO_3 , 15 mM MgCl_2 for 10 min, and then duplicate aliquots were used to measure RuBisCO activity by the [^{14}C]CABP assay (10 or 30 μM) (Ruuska *et al.*, 1998) in the presence of 1 mM DTT or 5 mM H_2O_2 for 30 min to reduce or oxidize RuBisCO, respectively. To minimize the effects of excess DTT or H_2O_2 , each reaction solution was diluted 20-fold with 50 mM EPPS-NaOH, pH 8.0, 20 mM MgCl_2 , 20 mM NaHCO_3 , 1 mM EDTA and then concentrated on an Amicon Ultra-15 Centrifugal Filter Unit (Merck Millipore, Burlington, MA, USA). The dilution/concentration process was repeated before the use.

The carboxylation rate was measured with the NADH-coupled spectrophotometric assay at 25°C by measuring the absorption at 340 nm with spectrophotometer (Sharwood *et al.*, 2016). The final concentrations of purified RuBisCO or rBSD2 in the assay solution were 80 nM (i.e. 10 nM per RuBisCO active site) and 40 nM, respectively. The assay was initiated by adding 0.5 mM ribulose 1,5-bisphosphate purified according to Kane *et al.* (1994) and Sharwood *et al.* (2016).

To estimate the ratio of oxidatively inactive to active RuBisCO in leaf, the frozen leaf was homogenized in glass homogenizer in ice-cold 50 mM Tris-HCl pH 7.6, 1 mM EDTA, 1% (w/v) polyvinylpyrrolidone, plant protease inhibitor cocktail (200 μM /25 ml solution) without DTT, and centrifuged at 16 000 g for 15 min at 4°C. The supernatants were incubated with or without 5 mM DTT (final concentration) on ice for 30 min, and RuBisCO carboxylation rate was measured with NADH-coupled spectrophotometric assay (Sharwood *et al.*, 2016) but without adding DTT.

DATA STATEMENT

All relevant data are provided within the manuscript and its supporting materials.

ACKNOWLEDGEMENTS

We are grateful to Spencer M. Whitney, Susanne von Caemmerer (both at The Australian National University) and Yoshiko Tateishi (Hiroshima University) for a gift of anti-BSD2 antibody and their advice and technical assistance with the *in vitro* RuBisCO activity assays. This work was supported in part by a JSPS KAKENHI Grant Number 26450081 (HS), 16H06552 (WY), A-STEP from the Japan Science and Technology Agency (HS), the Ministry of Education, Culture, Sports, Science and Technology (MEXT) as part of Joint Research Program implemented at the Institute of Plant Science and Resources, Okayama University in Japan (HS), grants from the Advanced Low Carbon Technology Research and Development Program from the Japan Science and Technology Agency (ST, TK, and HS), and the Join Usage/Research Center, Institute of Plant Science and Resources, Okayama University (HS), and the Japan Society for the Promotion of Science under the Japan-UK Research Cooperative Program from the Ministry of Education,

Culture, Sports, Science and Technology of Japan (TK). JT is supported by Research Fellowships for Young Scientists from JSPS, and FAB is supported by the Australian Government through the Australian Research Council Centre of Excellence for Translational Photosynthesis (CE1401000015).

AUTHOR CONTRIBUTION

ST and HS designed research; FAB, JT, MM, NS, ST, TK, KN, EM, CH, AM, and HS performed research; FAB, JT, ST, WY, SEM, YO, TT, SD, TK, WS, AS, and HS analyzed data; FAB, JT, ST, WY, SEM, YT, TT, WW, TK, WS, AS, and HS wrote the article.

CONFLICT OF INTEREST

The authors declare no conflict of interest.

SUPPORTING INFORMATION

Additional Supporting Information may be found in the online version of this article.

Figure S1. SDS-PAGE gel for RBCL and RBCS in leaves.

Figure S2. Measurements of total leaf area in Figure 1(d).

Figure S3. Comparisons of single leaf length and area in Figure 1(e).

Figure S4. Number of leaves in Figure 1(e).

Figure S5. Growth of 3-week-old plants on half-strength Murashige and Skoog medium plates.

Figure S6. Response of *A* to various *C_i* in leaves.

REFERENCES

- Aigner, H., Wilson, R.H., Bracher, A., Calisse, L., Bhat, J.Y., Hartl, F.U. and Hayer-Hartl, M. (2017) Plant RuBisCo assembly in *E. coli* with five chloroplast chaperones including BSD2. *Science*, **358**, 1272–1278.
- Albrecht, V., Ingenfeld, A. and Apel, K. (2008) Snowy cotyledon 2: the identification of a zinc finger domain protein essential for chloroplast development in cotyledons but not in true leaves. *Plant Mol. Boil.* **66**, 599–608.
- Balmer, Y., Vensel, W.H., Tanaka, C.K., Hurkman, W.J., Gelhaye, E., Rouhrie, N. and Buchanan, B.B. (2004) Thioredoxin links redox to the regulation of fundamental processes of plant mitochondria. *Proc. Natl. Acad. Sci. USA*, **101**, 2642–2647.
- Brutnell, T.P., Sawers, R.J., Mant, A. and Langdale, J.A. (1999) BUNDLE SHEATH DEFECTIVE2, a novel protein required for post-translational regulation of the *rbcL* gene of maize. *Plant Cell*, **11**, 849–864.
- Clough, S.J. and Bent, A.F. (1998) Floral dip: a simplified method for *Agrobacterium*-mediated transformation of *Arabidopsis thaliana*. *Plant J.* **16**, 735–743.
- Conlan, B., Birch, R., Kelso, C., Holland, S., De Souza, A.P., Long, S.P., Beck, J.L. and Whitney, S.M. (2018) BSD2 is a Rubisco-specific assembly chaperone, forms intermediary hetero-oligomeric complexes, and is nonlimiting to growth in tobacco. *Plant, Cell Environ.* <https://doi.org/10.1111/pce.13473>.
- de Crouy-Chanel, A., Kohiyama, M. and Richarme, G. (1995) A novel function of *Escherichia coli* chaperone DnaJ protein-disulfide isomerase. *J. Biol. Chem.* **270**, 22669–22672.
- Dietz, K.J., Turkan, I. and Krieger-Liszka, A. (2016) Redox and reactive oxygen species-dependent signaling into and out of the photosynthesizing chloroplast. *Plant Physiol.* **171**, 1541–1550.
- Doron, L., Segal, N., Gibori, H. and Shapira, M. (2014) The BSD2 ortholog in *Chlamydomonas reinhardtii* is a polysome-associated chaperone that co-migrates on sucrose gradients with the *rbcL* transcript encoding the Rubisco large subunit. *Plant J.* **80**, 345–355.
- Foyer, C.H. and Noctor, G. (2011) Ascorbate and glutathione: the heart of the redox hub. *Plant Physiol.* **155**, 2–18.
- Fristedt, R., Williams-Carrier, R., Merchant, S.S. and Barkan, A. (2014) A thylakoid membrane protein harboring a DnaJ-type zinc finger domain is

- required for photosystem I accumulation in plants. *J. Biol. Chem.* **289**, 30657–30667.
- García-Ferris, C. and Moreno, J.** (1993) Redox regulation of enzymatic activity and proteolytic susceptibility of ribulose-1, 5-bisphosphate carboxylase/oxygenase from *Euglena gracilis*. *Photosynth. Res.* **35**, 55–66.
- Hartings, S., Paradies, S., Karnuth, B., Einfeld, S., Mehling, J., Wolff, C., Levey, T., Westhoff, P. and Meierhoff, K.** (2017) The DnaJ-like zinc-finger protein HCF222 is required for thylakoid membrane biogenesis. *Plant Physiol.* **74**, 1807–1824.
- Ishida, H., Shimizu, S., Makino, A. and Mae, T.** (1998) Light-dependent fragmentation of the large subunit of ribulose-1, 5-bisphosphate carboxylase/oxygenase in chloroplasts isolated from wheat leaves. *Planta*, **204**, 305–309.
- Irihimovitch, V. and Shapira, M.** (2000) Glutathione redox potential modulated by reactive oxygen species regulates translation of Rubisco large subunit in the chloroplast. *J. Biol. Chem.* **275**, 16289–16295.
- Kane, H.J., Viil, J., Entsch, B., Paul, K., Morell, M.K. and Andrews, T.J.** (1994) An improved method for measuring the CO₂/O₂ specificity of ribulosebisphosphate carboxylase-oxygenase. *Funct. Plant Biol.* **21**, 449–461.
- Lemaire, S.D., Guillon, B., Le Maréchal, P., Keryer, E., Miginiac-Maslow, M. and Decottignies, P.** (2004) New thioredoxin targets in the unicellular photosynthetic eukaryote *Chlamydomonas reinhardtii*. *Proc. Natl Acad. Sci. USA*, **101**, 7475–7480.
- Lu, Y., Hall, D.A. and Last, R.L.** (2011) A small zinc finger thylakoid protein plays a role in maintenance of photosystem II in *Arabidopsis thaliana*. *Plant Cell*, **23**, 1861–1875.
- Marcus, Y., Altman-Gueta, H., Finkler, A. and Gurevitz, M.** (2003) Dual role of cysteine 172 in redox regulation of ribulose 1,5-bisphosphate carboxylase/oxygenase activity and degradation. *J. Bacteriol.* **185**, 1509–1517.
- Marín-Navarro, J. and Moreno, J.** (2003) Modification of the proteolytic fragmentation pattern upon oxidation of cysteines from ribulose 1, 5-bisphosphate carboxylase/oxygenase. *Biochemistry*, **42**, 14930–14938.
- Marín-Navarro, J. and Moreno, J.** (2006) Cysteines 449 and 459 modulate the reduction-oxidation conformational changes of ribulose 1,5-bisphosphate carboxylase/oxygenase and the translocation of the enzyme to membranes during stress. *Plant, Cell Environ.* **29**, 898–908.
- Moreno, J. and Spreitzer, R.J.** (1999) C172S substitution in the chloroplast-encoded large subunit affects stability and stress-induced turnover of ribulose-1, 5-bisphosphate carboxylase/oxygenase. *J. Biol. Chem.* **274**, 26789–26793.
- Moreno, J., García-Murria, M.J. and Marín-Navarro, J.** (2008) Redox modulation of Rubisco conformation and activity through its cysteine residues. *J. Exp. Bot.* **59**, 1605–1614.
- Muranaka, A., Watanabe, S., Sakamoto, A. and Shimada, H.** (2012) Arabidopsis cotyledon chloroplast biogenesis factor CYO1 uses glutathione as an electron donor and interacts with PSI (A1 and A2) and PSII (CP43 and CP47) subunits. *J. Plant Physiol.* **169**, 1212–1215.
- Nakagawa, T., Kurose, T., Hino, T., Tanaka, K., Kawamukai, M., Niwa, Y., Toyooka, K., Matsuoka, K., Jinbo, T. and Kimura, T.** (2007) Development of series of gateway binary vectors, pGWBs, for realizing efficient construction of fusion genes for plant transformation. *J. Biosci. Bioeng.* **104**, 34–41.
- Nakano, R., Ishida, H., Makino, A. and Mae, T.** (2006) In vivo fragmentation of the large subunit of ribulose-1,5-bisphosphate carboxylase by reactive oxygen species in an intact leaf of cucumber under chilling-light conditions. *Plant Cell Physiol.* **47**, 270–276.
- Parry, M.A., Andralojc, P.J., Scales, J.C., Salvucci, M.E., Carmo-Silva, A.E., Alonso, H. and Whitney, S.M.** (2013) Rubisco activity and regulation as targets for crop improvement. *J. Exp. Bot.* **64**, 717–730.
- Peltier, J.B., Cai, Y., Sun, Q., Zabrouskov, V., Giacomelli, L., Rudella, A., Ytterberg, A.J., Rutschow, H. and van Wijk, K.J.** (2006) The oligomeric stromal proteome of *Arabidopsis thaliana* chloroplasts. *Mol. Cell. Proteomics*, **5**, 114–133.
- Portis, A.R.** (2003) Rubisco activase–Rubisco's catalytic chaperone. *Photosynth. Res.* **75**, 11–27.
- Ranty, B., Lorimer, G. and Gutteridge, S.** (1991) An intra-dimeric crosslink of large subunits of spinach ribulose-1,5-bisphosphate carboxylase/oxygenase is formed by oxidation of cysteine 247. *Eur. J. Biochem.* **200**, 353–358.
- Raturi, A. and Mutus, B.** (2007) Characterization of redox state and reductase activity of protein disulfide isomerase under different redox environments using a sensitive fluorescent assay. *Free Radic. Biol. Med.* **43**, 62–70.
- Ruuska, S., Andrews, T.J., Badger, M.R., Hudson, G.S., Laisk, A., Price, G.D. and von Caemmerer, S.** (1998) The interplay between limiting processes in C3 photosynthesis studied by rapid-response gas exchange using transgenic tobacco impaired in photosynthesis. *Funct. Plant Biol.* **25**, 859–870.
- Sage, R.F., Way, D.A. and Kubien, D.S.** (2008) Rubisco, Rubisco activase, and global climate change. *J. Exp. Bot.* **59**, 1581–1595.
- Scales, J.C., Parry, M.A.J. and Salvucci, M.E.** (2014) A non-radioactive method for measuring Rubisco activase activity in the presence of variable ATP: ADP ratios, including modifications for measuring the activity and activation state of Rubisco. *Photosynth. Res.* **119**, 355–365.
- Sharkey, T.D., Bernacchi, C.J., Farquhar, G.D. and Singsaas, E.L.** (2007) Fitting photosynthetic carbon dioxide response curves for C3 leaves. *Plant Cell Environ.* **30**, 1035–1040.
- Sharwood, R.E., von Caemmerer, S., Maliga, P. and Whitney, S.M.** (2008) The catalytic properties of hybrid Rubisco comprising tobacco small and sunflower large subunits mirror the kinetically equivalent source Rubiscos and can support tobacco growth. *Plant Physiol.* **146**, 83–96.
- Sharwood, R.E., Sonawane, B.V., Ghannoum, O. and Whitney, S.M.** (2016) Improved analysis of C4 and C3 photosynthesis via refined in vitro assays of their carbon fixation biochemistry. *J. Exp. Bot.* **67**, 3137–3148.
- Shimada, H., Mochizuki, M., Ogura, K., Froehlich, J.E., Osteryoung, K.W., Shirano, Y., Shibata, D., Masuda, S., Mori, K. and Takamiya, K.** (2007) Arabidopsis cotyledon-specific chloroplast biogenesis factor CYO1 is a protein disulfide isomerase. *Plant Cell*, **19**, 3157–3169.
- Sudhani, H.P. and Moreno, J.** (2015) Control of the ribulose 1, 5-bisphosphate carboxylase/oxygenase activity by the chloroplastic glutathione pool. *Arch. Biochem. Biophys.* **567**, 30–34.
- Tang, W. and Wang, C.C.** (2001) Zinc fingers and thiol-disulfide oxidoreductase activities of chaperone DnaJ. *Biochemistry*, **40**, 14985–14994.
- Tanz, S.K., Kilian, J., Johnsson, C., Apel, K., Small, I., Harter, K., Wanke, D., Pogson, B. and Albrecht, V.** (2012) The SCO2 protein disulfide isomerase is required for thylakoid biogenesis and interacts with LHCB1 chlorophyll a/b binding proteins which affects chlorophyll biosynthesis in Arabidopsis seedlings. *Plant J.* **69**, 743–754.
- Tominaga, J., Mizutani, H., Horikawa, D., Nakahara, Y., Takami, T., Sakamoto, W., Sakamoto, A. and Shimada, H.** (2016) Rice CYO1, an ortholog of *Arabidopsis thaliana* cotyledon chloroplast biogenesis factor AtCYO1, is expressed in leaves and involved in photosynthetic performance. *J. Plant Physiol.* **207**, 78–83.
- Walker, B., Ariza, L.S., Kaines, S., Badger, M.R. and Cousins, A.B.** (2013) Temperature response of in vivo Rubisco kinetics and mesophyll conductance in *Arabidopsis thaliana*: comparisons to *Nicotiana tabacum*. *Plant Cell Environ.* **36**, 2108–2119.
- Whitney, S.M., Houtz, R.L. and Alonso, H.** (2011) Advancing our understanding and capacity to engineer nature's CO₂-sequestering enzyme. *Rubisco. Plant Physiol.* **155**, 27–35.
- Wostrikoff, K. and Stern, D.** (2007) Rubisco large-subunit translation is autoregulated in response to its assembly state in tobacco chloroplasts. *Proc. Natl Acad. Sci. USA*, **104**, 6466–6471.
- Zaffagnini, M., Bedhomme, M., Lemaire, S.D. and Trost, P.** (2012) The emerging roles of protein glutathionylation in chloroplasts. *Plant Sci.* **185**, 86–96.